Physica Medica 60 (2019) 168–173

Contents lists available at ScienceDirect

Physica Medica

journal homepage: www.elsevier.com/locate/ejmp

Technical note

An advanced junction concept in pediatric craniospinal irradiation by proton pencil beam scanning

Francesco Fellin, Francesco Fracchiolla, Barbara Rombi, Mirko Lipparini, Sabina Vennarini, Paolo Farace*

From Proton Therapy Center, Hospital of Trento, Azienda Provinciale per I Servizi Sanitari (APSS), Trento 38122, Italy

ARTICLE INFO

Keywords:
Craniospinal irradiation
Proton therapy
Field junction

ABSTRACT

Purpose: To present an advanced junction concept in craniospinal irradiation (CSI) by proton pencil beam scanning (PBS).

Materials and methods: In PBS CSI, whole brain irradiation (WBI) is commonly delivered by opposed lateral-beams, whereas spine irradiation is delivered by posterior entrances. Since lateral-beams would cross a large portion of the patient at the shoulder level, the junction between WBI and spine irradiation cannot extend below that level, thus the size of the lateral-beams needs to be limited and the number of required isocenters can increase. To overcome such limitation, a *pseudo-junction* was introduced below the posterior fossa, to turn in this region the WBI beam arrangement to a single posterior beam pointed at the same isocenter, that was matched to the posterior spinal beam more caudally, below shoulder level, in the *true-junction*. After assessing robustness of the technique to range and setup uncertainties, twenty-three treated patients were reviewed to estimate the percentage that might benefit of being treated by two instead of three isocenters.

Results: Target coverage at the junction levels resulted robust, with D95% > 95% on *pseudo-junction* and D95% > 90% on the *true-junction*. By the advanced junction concept, 91% of patients might by treated with only two isocenters, whereas, by the conventional method, 83% of patients required three isocenters.

Conclusion: With the presented junction concept the number of isocenters can be reduced, with a consequent relevant reduction of treatment time, which is particularly valuable in the management of pediatric patients under anesthesia.

1. Introduction

Medulloblastoma survivors have often significant adverse late effects involving heart, lungs, thyroid, growth of vertebral bodies, reproductive organs and risk of second neoplasm after irradiation of the spine as part of craniospinal irradiation (CSI). Proton therapy is emerging as the preferred treatment modality for CSI in pediatric patients [1,2], due to its physical characteristic and limited exit dose allowing to spare normal tissue. Since proton pencil beam scanning (PBS) is becoming more widely available, increasing precision of dose delivery and reducing contamination from secondary particles, with a low out-of-field dose and associated risk of radiation-induced cancer [3], PBS methods has been proposed for CSI [4,5].

A technical issue is on the number of isocenters to be used to treat the whole cranio-spinal axis. Due to limited field-size along the cranio-caudal direction, multiple isocenters are required. In details, in the beam arrangements proposed for whole brain irradiation (WBI) opposed lateral beams are commonly adopted, angled at most 15–20° to the posterior, allowing lens-sparing and robust coverage of the cribriform plate [4–7]. However, lateral beams entail anatomical limitation in the upper junction at the level of the shoulder. In fact, below that level these beams would undesirably cross a large portion of the patient, confining the junction volume between brain beams and the spinal beam in the neck area and disallowing the use of the full field size of the brain beams. This limitation can produce an increased number of isocenters (in most of the cases from two to three) to treat the whole cranio-spinal axis. Since increased treatment complexity and increased treatment delivering time is a direct consequence of an higher number of isocenters, any method to reduce complexity is valuable, particularly in the treatment of pediatric patients under anesthesia.

The present technical note describes an advanced junction concept in supine position, which allows to fully exploit the maximum field-size of cranial beams to reduce the number of required isocenters in most of the pediatric patients.

* Corresponding author at: Proton therapy Unit – Hospital of Trento, Via del Desert, 14, 38122 Trento, Italy.
E-mail address: paolofarace@gmail.com (P. Farace).

https://doi.org/10.1016/j.ejmp.2019.04.002
Received 21 December 2018; Received in revised form 3 April 2019; Accepted 6 April 2019
Available online 09 April 2019

2. Materials and methods

The method presented in the following is an extension of the CSI technique we are applying in patients affected by high-risk medulloblastoma that was comprehensively described in a previous study [5]. CSI was delivered in supine position, that is better tolerated and more stable and allows anesthesiologist direct access to the patient's oral cavity and airways. The total dose (3600 cGy RBE in 20 fractions) was delivered in two sequential phases. In the first phase (1980 cGy RBE in 11 fractions) the spinal clinical target volume (CTV_I) included the whole vertebral body, subarachnoid space and spinal nerve roots. In the second phase (1620 cGy RBE in 9 fractions) the spinal CTV_{II} included only subarachnoid space and laterally spinal nerve roots. We are adopting a two-phase regime in high-risk patients to limit unnecessary dose to normal tissues and reduce toxicities, while delivering enough dose to the ossification centers into the vertebral bodies to avoid growth impairment.

To obtain PTV_I, the CTV_I was expanded in the brain by 4 mm isotropically, and in the spine by 3 mm antero-posteriorly, by 5 mm cranio-caudally and by 5 mm laterally. To obtain PTV_{II}, the CTV_{II} was expanded in the brain by 4 mm isotropically and in the spine by 5 mm isotropically.

As in [5], field arrangement included i) two lateral plus a posterior beam (three-beam arrangement) on a common isocenter for WBI and ii) one adjacent posterior beam on caudal isocenter point to treat the spine. Single-field optimization (SFO) approach was applied. Field junction were obtained by a gradient-optimized method [8], using ancillary beams to produce it at the treatment planning system [9]. The effect on proton range due to the presence of the couch along the beam path in posterior beams was previously characterized [10].

Treatment plans were calculated and optimized in RayStation [11] (RaySearch Laboratories AB, Stockholm, Sweden), considering a constant RBE of 1.1 and using a Monte Carlo dose-engine to compute dose distribution.

Due to limited field size along the cranio-caudal direction (40 cm in our system) and the limitation posed by the use of lateral beams adopted for WBI, at least three isocenters are often required to treat the whole cranio-spinal axis, as it has been previously reported [4,5,12,13]. To overcome this limitation, an advanced junction concept is proposed. A *pseudo-junction* region was introduced below the posterior fossa, to turn in this region the brain beam arrangement from three-beam to a single posterior beam, still pointing on the common isocenter. Whereas WBI was equally delivered by the three SFO beams, with each beam uniformly delivering 33% of the prescribed dose, at the caudal edge of the *pseudo-junction* region the dose is entirely delivered by the posterior beam. In such a way the *true-junction*, where adjacent beams pointing at different isocenters are matched, can be planned between posterior beams only, without any anatomical limitation. Thus the *true-junction*, can be placed more caudally, fully exploiting the maximum field size of the brain posterior beam.

In details (see Fig. 1), in the planning procedure the upper isocenter (ISO1) was positioned as caudal as possible, compatible with the limitation of the on-board imaging system. In our system the field of view of the on-board flat panel covers around 33 cm in the cranio-caudal direction. Since for a better positioning of the patient the whole skull should be included in the image, the position of ISO1 was fixed at 16 cm from the top of the head. The position of the lower isocenter (ISO2) was defined by the relationship: Ls = 3Xo-Lj, where Ls was the distance between ISO1 and the end of the whole target and Lj was the length of the *true-junction* volume, which is typically chosen around 6–8 cm, and in this patient was around 7 cm. Xo define the position of ISO2. After expansion of CTV_I and CTV_{II}, both PTV_I (Fig. 1A) and PTV_{II} (Fig. 1B) need to be subdivided in five adjacent sub-volumes from top to bottom, including a *pseudo-junction* and a *true-junction* volumes. The *pseudo-junction* PTV originated from the foramen magnum and extended 3 cm caudally and the *true-junction* PTV extended form ISO1 + Xo-Lj to ISO1 + Xo.

To assess the impact of uncertainties in the *pseudo-junction* region, combinations of possible range and setup errors were simulated in a representative patient and robustness analysis was performed. Specifically, range uncertainty due to CT calibration errors was considered by scaling the mass density on the treatment volume by ± 3.5%, while to account for setup errors different shifts of the isocenter (3 and 5 mm) were tested. Both combined and individual range/setup errors were considered.

Additionally, robustness analysis was performed on the true-junction, investigating the impact of uncorrelated shifts between the two posterior beams with different isocenters that deliver the dose in this portion of the CTVs. In this case the robustness analysis consisted in the calculation of perturbed doses for the brain posterior beam, obtained by ± 3 mm shift in the cranio-caudal and by ± 5 mm in the lateral direction, combined with the corresponding uncorrelated shifts of the spinal beam.

Finally, to assess the impact of such advanced approach, twenty-three patients previously treated by a standard junction method were reviewed to estimate the percentage of patients that might benefit of being treated by two isocenters only using the advanced junction concept.

3. Results and discussion

In previous methods the transition from the brain beams to the spinal beam occurred at the same position for all beams, i.e. in the same junction volume. Thus to avoid crossing the shoulder area with the lateral beams, the junction volume between brain beams and the spinal beam has to be in the neck area, disallowing the use of the full field size of the brain beams. For some patients this requires an additional spinal beam.

The advanced junction approach allowed to overcome such limitation, as shown in Figs. 2 and 3. Treatment planning was obtained in different steps, using ancillary beams (more details on this gradient-optimized method were previously reported [5,9]) to obtain a linear dose gradient along the junctions (Fig. 2A). WBI was delivered with equal contribution by three brain beams, two lateral and one posterior using a common isocenter, with each beam uniformly delivering 33% of the prescribed dose (Fig. 2B). The posterior brain beam contributes 1/3 of the total dose in the brain and changes in the *pseudo-junction* volume so that at its caudal edge the 100% dose is entirely delivered by the posterior brain beam only (Fig. 2C). The posterior brain beam outreaches to the spine as far as possible to the caudal direction using the full field size, allowing the *true-junction* to be placed more caudally, regardless the level of the shoulders. The same procedure was repeated to plan both the first phase of the treatment on PTV_I (Fig. 2) and the second phase of the treatment on PTV_{II} (Fig. 3).

Worst-case robustness analysis at the *pseudo-junction*, i.e. at the volume of CTVs included in the pseudo-junction, is reported in Table 1 for a representative patient, assuming ± 3.5% range uncertainties and variable (3 or 5 mm) setup errors. Both combined range/setup errors and individual errors were reported. The values investigated to account for the setup errors corresponds to the margin we are currently adopting to obtain the PTVs spine from the corresponding CTVs. They differ from the 4 mm uniform margin adopted in our first treatments [5]. These values were modified to account for the experience obtained in daily alignment by kilo-voltage imaging, considering the different CTVs and directions. CTV_I including the whole vertebral body is expanded by 3 mm anteriorly as it was proposed by other authors [4] to account for set-up errors, but with greater margin (5 mm) laterally, since in this direction some difficulties were encountered in daily kilo-voltage alignment. Differently from what it was, a fixed 3 mm margin is used in the beam direction (antero-posterior), without computing the additional expansion suggested by the same authors [4] to account for the distal range uncertainty. Such smaller margin improved

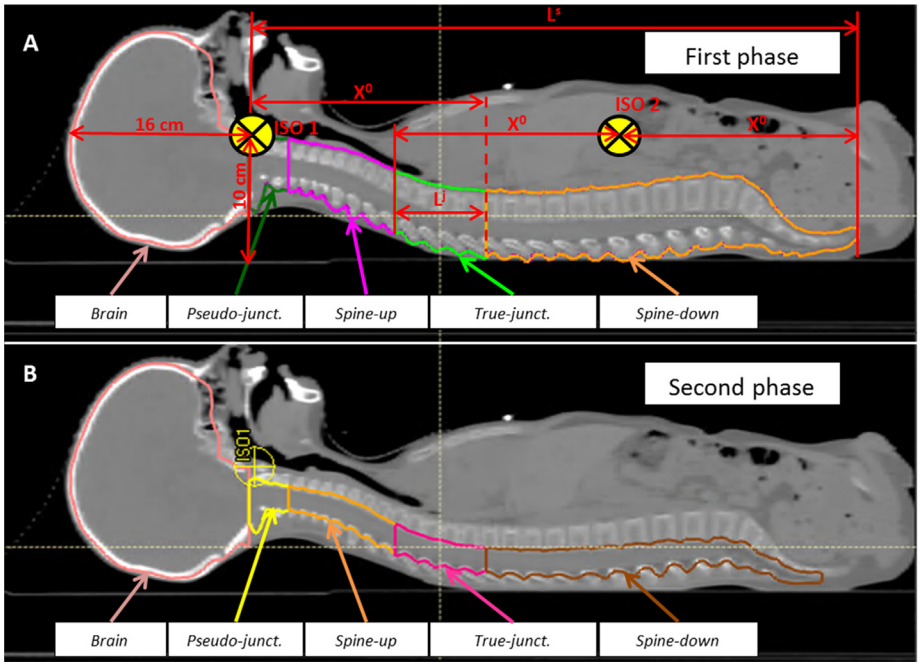

Fig. 1. Isocenters and sub-volumes definition. (A) The isocenter ISO1 was at 16 cm from the top of the head, compatible with the limitation of the on-board imaging system. The position of ISO2 was defined by the relationship: Ls = 3Xo-Lj, where Ls was the distance between ISO1 and the end of the whole target and Lj was the length of the true-junction volume (around 7 cm in this patient). Xo define the position of ISO2. After expansion of CTV_I and CTV_{II}, both PTV_I (A) and PTV_{II} (B) need to be subdivided in five different sub-volumes. The *pseudo-junction* PTV originated from the foramen magnum and extended 3 cm caudally. The *true junction* PTV extended form ISO1 + Xo-Lj to ISO1 + Xo.

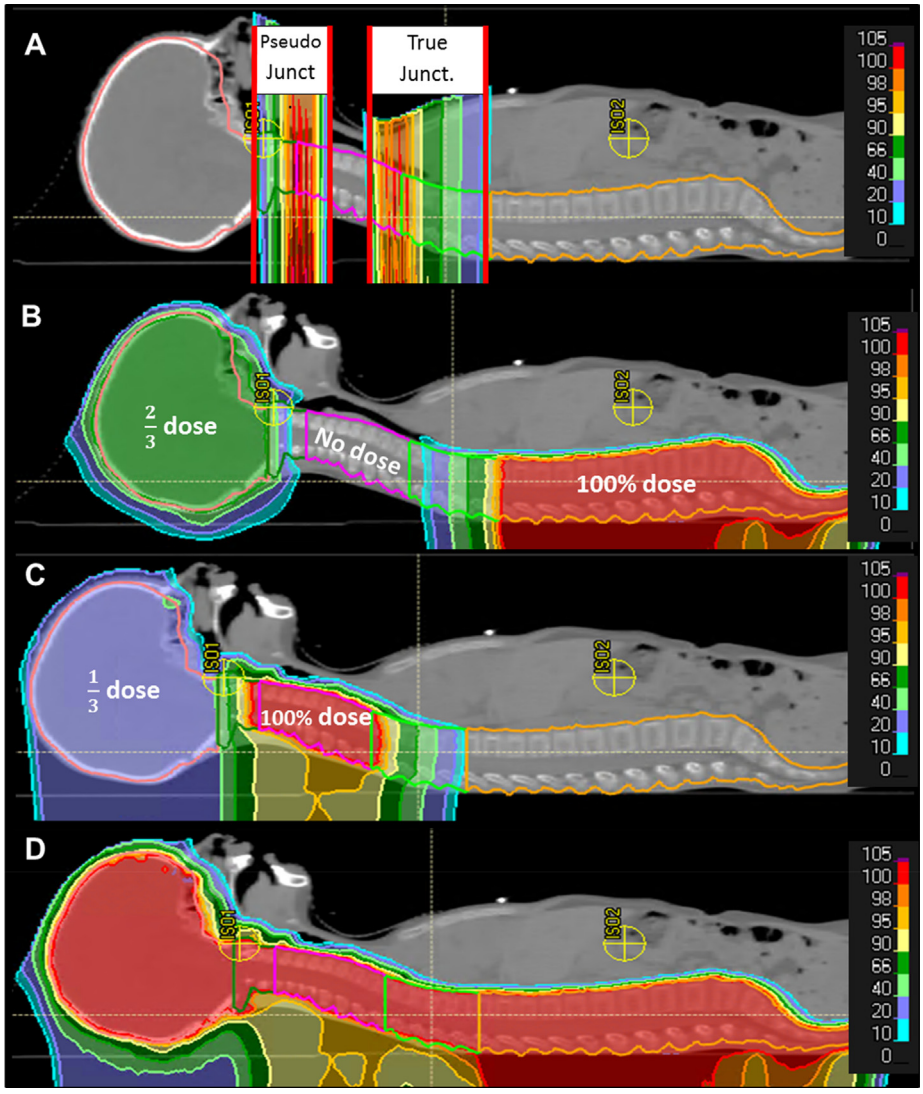

Fig. 2. Treatment planning by the advanced junction technique. Pseudo- and true- junctions were planned by a gradient-optimized method using ancillary beams, that produced a linear dose gradient along the junctions (A). The ancillary beams were used in the background during the inverse plan optimization of the lateral and spinal beams, and then deleted. The obtained dose delivered by the two lateral beams for WBI (delivering together 2/3 of the prescribed dose), plus the posterior spinal beam is shown in (B). With this dose distribution as a background, the dose to be delivered by the posterior brain beam is obtained (C). The total dose distribution is shown in (D). Dose are reported as percentage of the prescription dose (1980 cGy RBE).

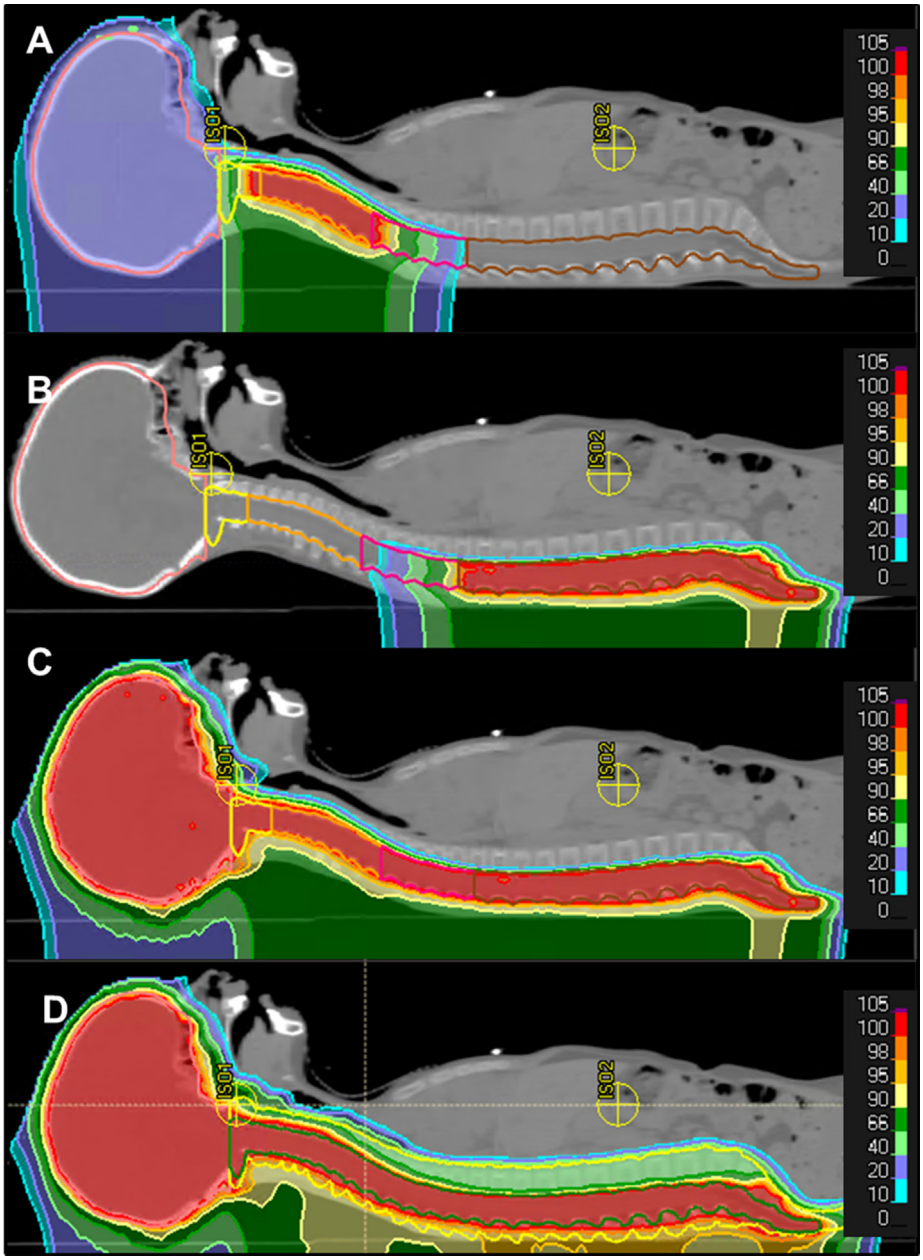

Fig. 3. Treatment planning of the second phase. For the second phase, the same lateral brain beams of the first phase were used (not shown), plus newly optimized posterior brain beam (A) and posterior spinal beam (B). The obtained dose distribution allow to spare the vertebral bodies (C). The total dose distribution (first phase plus second phase) is also shown (D). Dose are reported as percentage of the prescription dose (in A-C 1620 cGy RBE; in D 3600 cGy RBE).

downstream organ at risk sparing and was supported by the results reported in Table 1**,** showing that range uncertainty had a minimal effect on the dose delivered to the pseudo- junction CTVs. Similar data on the effect of range uncertainty were observed on the other portion of CTV spine (not shown). Besides that, the vertebral bodies are not a tumor target, but they are irradiated to limit potential growth impairment. For this reason, the slight D95 < 95% under-dosage observed in the CTV_I covering the pseudo-junction in the first phase (worst case scenario D95 = 93.7% with setup and range errors ± 5 mm and ± 3.5% respectively) has negligible clinical impact. On the contrary, since CTV_{II} spine is a tumor target a greater margin was adopted, that allowed to always obtain on the pseudo-junction a dose coverage at the 95% level for the simulated errors (Table 1). The 5 mm margin applied on CTV_{II} was somehow intermediate between the 3 mm plus distal margin suggested in [4] and the 7 mm margin applied by passive scattering by other authors [14], who however accepted a 1–2 mm smaller distal margin in the cervical spine to spare the thyroid gland. On both CTV_I and CTV_{II} the margin applied along the cranio-caudal direction was 5 mm, which accounted for setup errors and potential correction of the relative position of the two isocenters. In fact, as previously reported [5], a maximum offset of 3 mm between adjacent isocenters was allowed during daily kilovoltage aligning.

The effect of this relative shift between isocenters, i.e. of uncorrelated offset between the corresponding beams, was investigated in details on the *true-junction* for the same representative patient (Table 2). The analysis was focused only on latero-lateral (LL) and cranio-caudal (CC) directions. The anterior-posterior direction was excluded as in this direction the two posterior beams cannot be shifted each other in our workflow [5]. For simplicity, range uncertainty was also excluded considering the low impact previously shown in Table 1. For the analysis, perturbed dose of the cranial posterior beam were computed selecting ± 3 mm shifts in CC direction (i.e. the maximal CC allowed

Table 1
Robustness analysis on pseudo-junction-CTV for a representative case.

Scenarios	First-phase*				Second-phase**	
	Pseudo-junction-CTV$_I$		Pseudo-junction-CTV$_{II}$		Pseudo-junction-CTV$_{II}$	
	D95(%)	D1(%)	D95(%)	D1(%)	D95(%)	D1(%)
Nominal	100.5	105.3	100.5	105.2	100.9	105.2
± 3 mm ± 3.5%[a]	96.7	108.0				
± 5 mm ± 3.5%[a]	93.7	108.9	97.1	110.2	95.1	109.0
± 3 mm[b]	98.5	106.8				
± 5 mm[b]	95.9	107.8	98.4	108.6	95.5	108.2
± 3.5%[c]	99.2	106.5	99.0	106.5	99.8	106.8

± 3 mm and ± 5 mm define the setup shift and ± 3.5% define the range uncertainty investigated in the robustness analysis.
* Worst case result reported as % of the prescribed dose (1980 cGy RBE).
** Worst case result reported as % of the prescribed dose (1620 cGy RBE).
[a] Combined range and setup errors were considered.
[b] Only setup errors were considered.
[c] Only range uncertainty was considered.

offset between adjacent isocenters, as above discussed) and ± 5 mm shifts in LL (the same value used for PTV expansion). For the caudal posterior beam additional uncorrelated shifts were computed to obtain combined scenarios, selecting those compatible with the constraint we are adopting during daily alignment (left columns in Table 2). As expected, the perturbed dose computed in the investigated scenarios confirmed that the maximum dose (D1) increased when the beams were shifted towards each other along the CC direction, while the target coverage (D95) has worsened when the beams were moved apart along the same direction. These results are compatible with the linear relationship linking the dose deviation in the junction with the ratio between the shift and junction length, previously suggested [4,9]. However, the CTV coverage at the D95 level was always above 90%, and the maximal D1 was around 110%, confirming the robustness of the method.

Finally, reviewing 23 treated patient, 21 patients (91%) might be treated with two isocenters with only 2 patients (9%) still requiring three isocenters due to target length, whereas by the conventional method only 4 patients (17%) were treated with two isocenters and 19 patients (83%) required three isocenters. By using only two isocenters a relevant reduction of session treatment time (> 30% in our practice) could be obtained, due to faster patient alignment and faster dose delivery.

In conclusion, by the advanced junction concept presented in this note, the number of isocenters could be reliably reduced in most of the patients, with a consequent reduction of the treatment session, which is valuable considering that many pediatric patients are treated under anesthesia.

Conflict of interest statement

Authors report no conflict of interest.

Table 2
Robustness analysis on true-junction-CTVs for a representative case.

Scenarios[§]				First-phase*				Second-phase**	
Brain		Spine		True-junction-CTV$_I$		True-junction-CTV$_{II}$		True-junction-CTV$_{II}$	
LL mm	CC mm	LL mm	CC mm	D95 %	D1 %	D95 %	D1 %	D95 %	D1 %
0	0	0	0	100.2	105.4	100.9	105.2	99.4	104.1
0	0	5	3	102.7	109.7	104.1	109.7	103.2	109.6
0	0	5	−3	95.0	103.1	96.3	102.5	94.7	103.2
0	0	−5	3	103.5	109.9	104.3	109.8	103.3	110.1
0	0	−5	−3	95.7	103.1	96.5	102.5	95.0	103.4
5	3	0	0	93.3	102.0	96.5	101.1	94.3	101.5
5	−3	0	0	101.1	110.3	103.1	108.8	102.4	108.5
−5	3	0	0	94.0	102.1	96.6	101.3	95.0	101.7
−5	−3	0	0	101.7	110.1	103.3	109.2	103.2	108.5
5	3	5	3	94.2	105.9	100.0	105.2	98.5	104.4
5	−3	5	−3	94.3	106.0	100.3	104.7	98.1	104.6
−5	3	−5	3	96.8	106.1	100.5	105.2	99.6	104.5
−5	−3	−5	−3	97.0	106.0	100.6	105.3	98.8	105.0
−5	3	0	6	102.4	110.3	104.3	109.4	103.5	108.6
−5	−3	0	−6	94.0	103.8	96.6	103.5	94.4	104.3
5	3	0	6	101.6	110.3	104.2	109.4	102.8	108.8
5	−3	0	−6	92.9	103.7	96.4	103.0	93.7	104.0
				Min	**Max**	**Min**	**Max**	**Min**	**Max**
				92.9	110.3	96.3	109.8	93.7	110.1

* Worst case result reported as % of the prescribed dose (1980 cGy RBE).
** Worst case result reported as % of the prescribed dose (1620 cGy RBE).
[§] Tested combination of scenarios with uncorrelated shifts along the cranio-caudal (CC) and the lateral (LL) directions for the brain and the spine beams respectively.

References

[1] Yock TI, Yeap BY, Ebb DH, Weyman E, Eaton BR, Sherry NA, et al. Long-term toxic effects of proton radiotherapy for paediatric medulloblastoma: a phase 2 single-arm study. Lancet Oncol 2016;17(3):287–98.

[2] Ho ESQ, Barrett SA, Mullaney LM. A review of dosimetric and toxicity modeling of proton versus photon craniospinal irradiation for pediatrics medulloblastoma. Acta Oncol 2017;56(8):1031–42.

[3] Ardenfors O, Dasu A, Lillhök J, Persson L, Gudowska I. Out-of-field doses from secondary radiation produced in proton therapy and the associated risk of radiation-induced cancer from a brain tumor treatment. Phys Med 2018;53:129–36.

[4] Lin H, Ding X, Kirk M, Liu H, Zhai H, Hill-Kayser CE, et al. Supine craniospinal irradiation using a proton pencil beam scanning technique without match line changes for field junctions. Int J Radiat Oncol Biol Phys 2014;90(1):71–8.

[5] Farace P, Bizzocchi N, Righetto R, Fellin F, Fracchiolla F, Lorentini S, et al. Supine craniospinal irradiation in pediatric patients by proton pencil beam scanning. Radiother Oncol 2017;123:112–8.

[6] Cochran DM, Yock TI, Adams JA, Tarbell NJ. Radiation dose to the lens during craniospinal irradiation-an improvement in proton radiotherapy technique. Int J Radiat Oncol Biol Phys 2008;70(5):1336–42.

[7] Giebeler A, Newhauser WD, Amos RA, Mahajan A, Homann K, Howell RM. Standardized treatment planning methodology for passively scattered proton craniospinal irradiation. Radiat Oncol 2013;3(8):32.

[8] Wang K, Meng H, Chen J, Zhang W, Feng Y. Plan quality and robustness in field junction region for craniospinal irradiation with VMAT. Phys Med 2018;48:21–6.

[9] Farace P, Vinante L, Ravanelli D, Bizzocchi N, Vennarini S. Planning field-junction in proton cranio-spinal irradiation – the ancillary-beam technique. Acta Oncol 2015;54(7):1075–8.

[10] Fellin F, Righetto R, Fava G, Trevisan D, Amelio D, Farace P. Water equivalent thickness of immobilization devices in proton therapy planning – modelling at treatment planning and validation by measurements with a multi-layer ionization chamber. Phys Med 2017;35:31–8.

[11] Bäumer C, Geismar D, Koska B, Kramer PH, Lambert J, Lemke M, et al. Comprehensive clinical commissioning and validation of the RayStation treatment planning system for proton therapy with active scanning and passive treatment techniques. Phys Med 2017;43:15–24.

[12] Stoker JB, Grant J, Zhu XR, Pidikiti R, Mahajan A, Grosshans DR. Intensity modulated proton therapy for craniospinal irradiation: organ-at-risk exposure and a low-gradient junctioning technique. Int J Radiat Oncol Biol Phys 2014;90(3):637–44.

[13] Seravalli E, Bosman M, Lassen-Ramshad Y, Vestergaard A, Oldenburger F, Visser J, et al. Dosimetric comparison of five different techniques for craniospinal irradiation across 15 European centers: analysis on behalf of the SIOP-E-BTG (radiotherapy working group). Acta Oncol 2018;57(9):1240–9.

[14] Barney CL, Brown AP, Grosshans DR, McAleer MF, de Groot JF, Puduvalli V, et al. Technique, outcomes, and acute toxicities in adults treated with proton beam craniospinal irradiation. Neuro Oncol 2014;16(2):303–9.